Presented at the National Bureau
of Standards - Ceramic Meeting,
Gaithersburg, Washington,
November 12, 1978

LBL-8608

# ABRASIVE WEAR IN CERAMICS: AN ASSESSMENT

A. G. Evans



January 1979

Prepared for the U. S. Department of Energy
under Contract W-7405-ENG-48



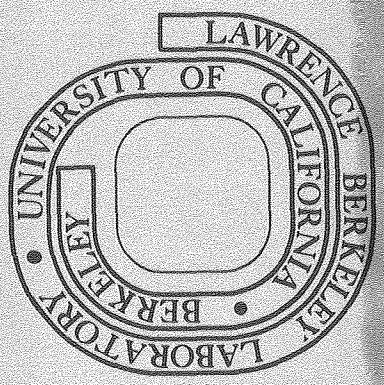

# ABRASIVE WEAR IN CERAMICS: AN ASSESSMENT

A. G. Evans

University of California
Berkeley, CA 94720

The mechanisms of material removal during abrasive wear have been examined, and preliminary analyses presented. Primary emphasis has been placed on the lateral fracture mechanism, in an attempt to elucidate both its realm of importance and the concomitant material removal rates. Thermal stresses induced by plastic penetration have also been shown to be a potential source of material removal, especially at low levels of the normal force.

## 1. Introduction

The abrasive wear of ceramics has been the subject of extensive empirical investigation [1].[1] For example, material removal rates have been measured on various materials as functions of the normal force, $P_n$, the horizontal (frictional) force, $P_\ell$, the wheel speed, etc. However, the detailed mechanisms of material removal have only been cursorily explored. Yet, some understanding of mechanisms is an essential prerequisite to optimization (especially for complex processes such as abrasive wear). The intent of the present paper is to examine possible mechanisms of abrasive material removal, as a prelude to suggesting research studies that should elucidate details of the various removal processes.

Several investigators [2-4] have recently recognized the important role of lateral fracture in abrasive material removal. This mechanism of wear is explored in some detail, to determine both its realm of importance and the parameters that might influence the removal rate. Other potential mechanisms of material removal are then examined to assess their significance as alternative or superposed influences.

## 2. Lateral Fracture Mechanisms

### 2.1 Regime of influence

Studies of indentation conducted under quasi-static [4], sliding [2,3] and impact conditions have indicated a threshold for lateral crack formation. A definition of this threshold is of great significance, because it defines the lower limit of pertinence of the lateral fracture mechanism of abrasive wear. A transition to another mechanism may also obtain under very severe grinding conditions [2]. However, this regime could be just

[1] Figures in brackets indicate the literature references at the end of this paper.

another manifestation of lateral cracking (perhaps involving a multiplicity of lateral cracks as observed during projectile impact [5]); consequently, this "transition" is not afforded specific consideration in the present analysis.

During "steady-state" grinding conditions, a ceramic will contain a distribution of microcracks, formed as a consequence of the stresses produced by the penetration of the grinding particles. These pre-existent microcracks are considered to be the sources of lateral fracture. The pre-existent microcracks will develop into lateral cracks when the grinding stresses attain the requisite level. The tensile stresses that induce lateral cracks develop primarily during load removal [6,7] (i.e. residual stresses), and exhibit a maximum either within the plastic zone (in work hardening materials) or at the elastic/plastic interface (in non-hardening materials). It has recently been demonstrated [8] that elastic/plastic indentation fields can be approximated in the immediate vicinity of the plastic zone by the elastic/plastic solution for a spherical cavity,† and remote from the indentation by the elastic solution for a half-space: the intermediate stresses being obtained by interpolation. This procedure also provides estimates of the residual tensile stress, $\sigma^R_{zz}$, obtained by subtracting the elastic unloading stresses from the elastic/plastic stresses at peak load. In particular, the residual stresses in the elastic zone (the zone of primary interest for fracture analysis [4]), are obtained at zero load by matching the elastic stress at the indenter interface, $\hat{\sigma}^e_{zz}$, to the equivalent elastic/plastic stress at peak penetration, a, (i.e. to the hardness H), viz;

$$\hat{\sigma}^e_{zz} = -\left(\frac{3H}{2}\right)\left(\frac{z}{\sqrt{u}}\right)^3\left[\frac{\hat{a}^2 u}{u^2 + \hat{a}^2 z^2}\right] \tag{1}$$

where

$$2u = r^2 + z^2 - \hat{a}^2 + \sqrt{(r^2 + z^2 - \hat{a}^2) + 4a^2 z^2}$$

and then subtracting this stress from the elastic/plastic stress, $\sigma^p_{zz}$;

$$\sigma^p_{zz} = -\left(\frac{\sigma_y}{6}\right)\left(\frac{r_p}{\sqrt{z^2 + r^2}}\right)^3\left[1 + 3\left(\frac{z^2 - r^2}{z^2 + r^2}\right)\right] \qquad (z > 0) \tag{2}$$

By noting that, $\sigma_y \sim H/3$ [4,6,10], and that, $r_p \sim \hat{a}$ [4,5], the residual stress $\sigma^R_{zz}$ at zero load becomes;

$$\sigma^R_{zz} \equiv \left(\sigma^p_{zz} - \hat{\sigma}^e_{zz}\right) \approx \left(\frac{H\hat{a}^2}{2}\right)\left\{\frac{3z^2}{\sqrt{u}(u^2 + \hat{a}^2 z^2)} - \frac{\hat{a}}{9(z^2 + r^2)^{3/2}}\left[1 + 3\left(\frac{z^2 - r^2}{z^2 + r^2}\right)\right]\right\} \tag{3}$$

†With the obvious exception of $\sigma_{zz}$ stresses near the surface, which are poorly predicted by the spherical cavity solution.

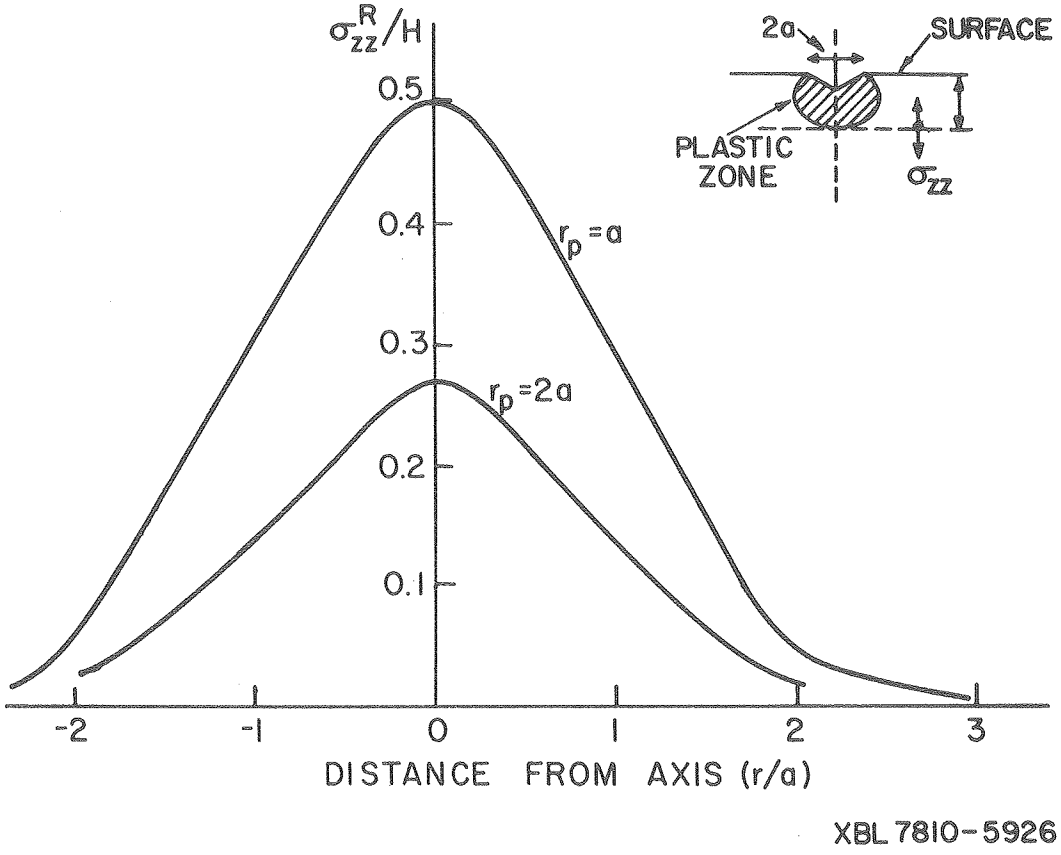


Fig. 1 The spatial dependence of the residual tensile stress along a plane through the intersection of the plastic zone with the penetration axis: the stresses were estimated from an analytic elastic/plastic solution for a spherical cavity and an elastic solution for a half space.

The peak axial value of this stress,

$$\hat{\sigma}^R_{zz} \approx H/2$$

occurs at the elastic/plastic interface, and is appreciably larger than the peak stress at maximum penetration [8] (~ H/12). Note, however, that $\hat{\sigma}^R_{zz}$ decreases rapidly as the relative plastic zone size increases, e.g. $\sigma^R_{zz} = 0.27H$ at $r_p = 2a$.

The spacial variation of the stress along a plane through the location of maximum tension is plotted in Fig. 1. The stresses can be approximated by

$$\begin{aligned} \sigma^R_{zz} &\approx \sigma(1 - r/2a) && (r < 2a) \\ \sigma^R_{zz} &= 0 && (r > 2a) \end{aligned} \tag{5}$$

where $\hat{\sigma}$ is the peak stress. A stress-intensity factor solution for an axisymmetric crack located in such a linearly varying stress field has recently been derived by Lawn and Evans [11]. This solution demonstrates the existence of an absolute minimum $P^*$ in the normal force required for crack activation. For the stress field represented by eq. (5), $P^*$ is given by

$$P^* = 14\xi^4 \beta K_c^4/H^3 \tag{6}$$

where $K_c$ is the toughness of the material, $\beta$ is a parameter related to the shape of the indenting particle [11] (e.g. $\beta = 2/\pi$ for a Vickers indenter) and $\xi = H/\hat{\sigma}$. In a material that contains a wide size distribution of pre-existent microcracks, there will be a relatively high probability of lateral crack nucleation at $P^*$. However, more generally, $P^*$ will need to be exceeded: by an amount related to the size range of microcracks in the vicinity of the indentation. The parameter $K_c^4/H^3$ in the expression for $P^*$ is considered to afford a reasonably accurate relative measure of the influence of the material variables on the fracture threshold, as indicated by recent observations on radial fracture [12]. However, the magnitudes of the coefficients - being strongly dependent on the value of the peak stress - could be appreciably in error and should only be regarded as order of magnitude estimates.

## 2.2 Material removal rates

The amount of material removed by the passage of each abrasive particle that exceeds the fracture threshold force $P^*$ is determined (in part) by the extent of the lateral fracture. Most observations of lateral fracture indicate that the fracture extent is related

to the extent of the prior radial fracture (4,5]; but the generality of this result has not been substantiated. Nevertheless, the present analysis of material removal rates will assume a relationship between lateral crack extension and the more extensively characterized radial crack extension, C. The average depth of the lateral cracks, $< h >$, also influences the material removal (Fig. 2a). The only available analysis of lateral crack depths indicates that $< h >$ is proportional to the plastic zone radius $r_p$. This relationship will also be assumed in the present analysis.

The maximum volume $\hat{V}_i$ of material that could be removed by the passage of an abrasive particle is (Fig. 2);

$$\hat{V}_i \approx 2 < h_i > C_i \ell_i \tag{7}$$

where $\ell_i$ is the distance of motion. This expression will be the basis for estimating variations in the material removal rate.

The plastic zone radius $r_p$ is related to the plastic contact radius a, under both dynamic [5] and quasi-static [4] conditions. We will use the direction proportionality, $r_p \propto a$, so that,

$$< h > \approx \psi a \tag{8}$$

where $\psi$ is a constant $\approx 1$. However, the radial crack extension C differs appreciably under quasi-static and dynamic conditions [5]: being more extensive (for the equivalent contact area) under dynamic conditions. For typical abrasive wear situations, both quasi-static and dynamic conditions can obtain. A preliminary analysis that embraces both quasi-static and dynamic influences is attempted herein. The analysis considers the extension of the lateral cracks normal to the motion of the abrading particle (Fig. 2a), since this distance defines the width of the potential material removal zone. The situation to be modelled is defined in Fig. 2b; it consists of an abrasive particle subjected to normal force $P_n$, moving with a prescribed lateral velocity $v_\ell$.

If the velocity $v_\ell$ is very low, the consequences of the lateral motion can be approximated by a quasi-static lateral force $P_\ell \equiv \mu P_n$ (where $\mu$ is a friction coefficient). Although this condition is rarely encountered, it is instructive to examine the influence of the lateral force, vis-a-vis the normal force. The normal force dictates the penetration according to the normal hardness relation [11];

$$H = P_n/\beta\pi a^2 \tag{9}$$

---

†A tenuous rationale for this observation is that the presence of the radial cracks enhances the stress intensity factor at lateral cracks toward the limit of their extension, by relaxing the circumferential constraint and permitting additional z-displacements.

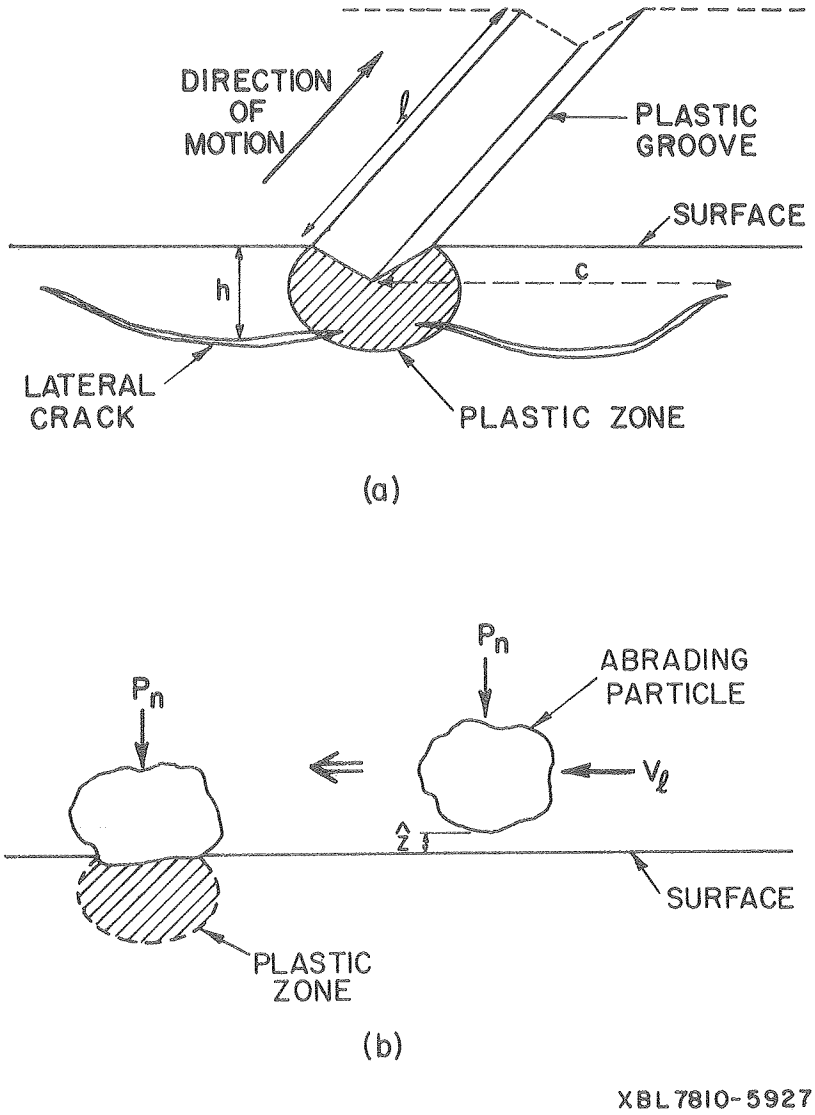


Fig. 2 a) A schematic indicating the nature of the lateral cracking that leads to material removal

b) A schematic indicating typical conditions that apply to an abrading particle during abrasive wear.

Both the lateral and normal forces are expected to influence the stress field. By analogy with the equivalent elastic problem [13], it is anticipated that the lateral force will tend to rotate the stress field in the direction of $P_\ell$, in the sense that the tension is enhanced behind the contact zone and suppressed ahead of the contact. But, there should be no appreciable influence on the stresses contained in the plane normal to $P_\ell$. The latter have the primary effect on the lateral crack extension normal to the motion of the abrading particle. It is thus concluded that under quasi-static conditions, the width of the lateral fracture zone should be relatively insensitive to the magnitude of the lateral force. The zone width may, therefore, be approximately characterized by a relation similar to that obtained for radial cracks under conditions of normal penetration; viz., for a Vicker's indenter [14],

$$C/a = F_1 \left[ (K_c/H\sqrt{a}), (H/E) \right] \tag{10a}$$

where $F_1$ is a function, which for $c/a \gtrsim 2$ reduces to;

$$F_1 \approx 0.29 \left( \frac{K_c}{H\sqrt{a}} \right)^{-2/3} \tag{10b}$$

giving;

$$C = \frac{0.29}{(\pi\alpha)^{2/3}} \left( \frac{\hat{P}}{K_c} \right)^{2/3} \tag{10c}$$

Combining equations (7), (8) and (10c) yields the quasi-static material removal rate;

$$\hat{V}_i^{\varepsilon} = \left[ \frac{0.58\psi}{(\pi\beta)^{7/6}} \right] \frac{\left( P_n \right)_i^{7/6}}{\left( K_c^{2/3} H^{1/2} \right)} \ell_i \tag{11}$$

More generally, the lateral motion of the abrading particle will lead to dynamic effects. These dynamic effects arise both from the prescribed motion $v_\ell$ of the particle, and from local instabilities. The instabilities occur following a fracturing event and result in an abrupt increase in the local particle velocity. They are manifested as the lateral force oscillations typically observed in studies of the motion of abrading particles. The impact events that result from the instabilities are likely to have impulse components both normal and parallel to the surface. The normal component will affect the penetration, but both components will influence the dynamic stress field. We will assume that, as in the quasi-static case, the lateral component of velocity does not generate stresses that significantly influence lateral crack extension in the direction of present interest (Fig. 2a). The effect of the normal particle velocity $v_n$ can then be assessed from experimental

results obtained for projectile impact [5];

$$C \approx \left[ r_p^2 v_n^2 / K_c \right]^{2/3} \tag{12}$$

where $r_p$ is the radius of the projectile and $\lambda$ is a constant. The normal component of the velocity acquired by the abrading particle depends on the magnitude of the normal force $P_n$ and the height $\hat{z}$ that the particle rises above the surface during the instability (Fig. 2b);

$$v_n^2 = 2P_n\hat{z}/m \tag{13}$$

Where m is the mass of the grinding wheel. The height $\hat{z}$ will be influenced by the detailed character of the instability, the imposed lateral velocity $v_\ell$ and the friction coefficient $\mu$. The influence of normal velocity on the extent of the fracture will be assumed in the present analysis to be equivalent to that found for projectile impact. This assumption is based on the premise that the stresses which influence the fracture relate to the conditions that prevail soon after initial contact:[5] as dictated by the impedence, the initial velocity mismatch and the dynamic hardness. Clearly, experimental studies of the velocity dependence of C are needed to assess the utility of this assumption. The crack extension obtained from eq. (12) is then;

$$C = \left[ \frac{P_n \hat{z}(v_\ell, \mu)}{K_c} \right]^{2/3} F(r_p, m) \tag{14}$$

where F is an undetermined function. It is interesting to note that the dependence on the normal force is identical to that obtained for quasi-static indentation (eq. 11). Now, assuming that eq. (9) still affords a reasonable estimate of the contact radius, equations (7), (9), and (14) can be combined to give;

$$\hat{V}_i^d = \left[ \frac{2\ F(r_p, m)}{(\pi\beta)^{1/2}} \right] \left[ \frac{(P_n)_i^{7/6}}{H^{1/2}} \right] \left[ \frac{\hat{z}(v_\ell, \mu)}{K_c} \right]^{2/3} \ell_i \tag{15}$$

This result is quite similar to the quasi-static result except that influences of the lateral velocity and the friction coefficient emerge, through the instability height $\hat{z}$. No information is presently available concerning the magnitude of the instability; this is clearly an important parameter for future study.

A comparison of the predictions of the present simplified analysis with available results should provide a basis for assessing the merits of this approach to abrasive material removal. The dependence of the lateral crack width on the normal force has previously been examined by Veldkamp et al [3] in MgZn ferrite, and shown to approximately conform with the predicted $P_n^{2/3}$ relation (Fig. 3). The dependence of the material removal

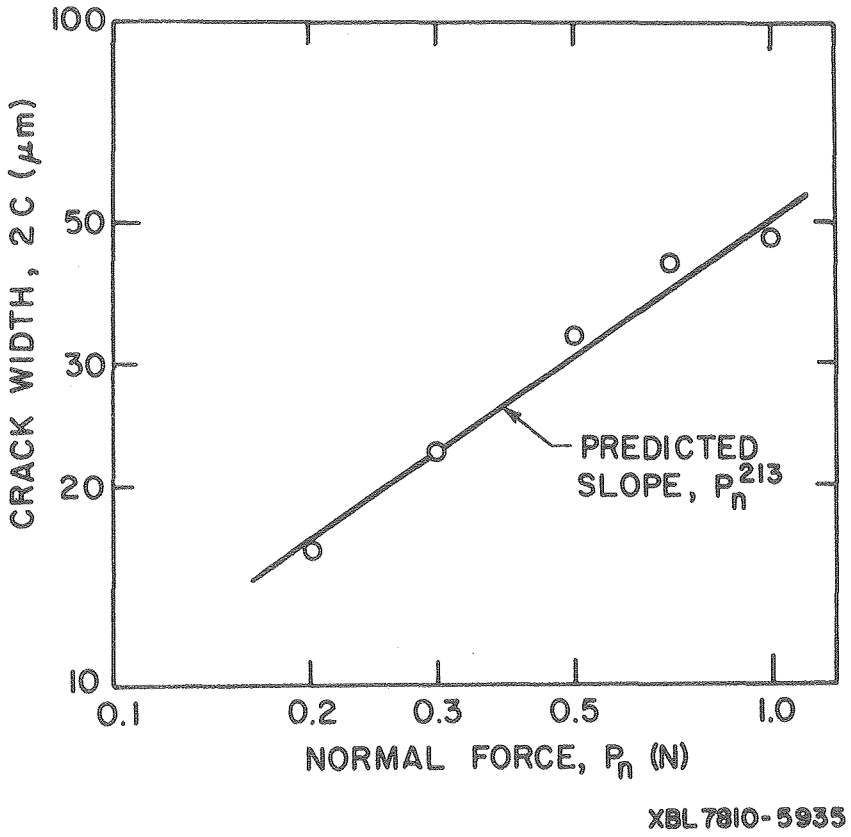


Fig. 3 A plot of the lateral crack width as a function of the normal force[3], indicating the $P_n^{2/3}$ relation.

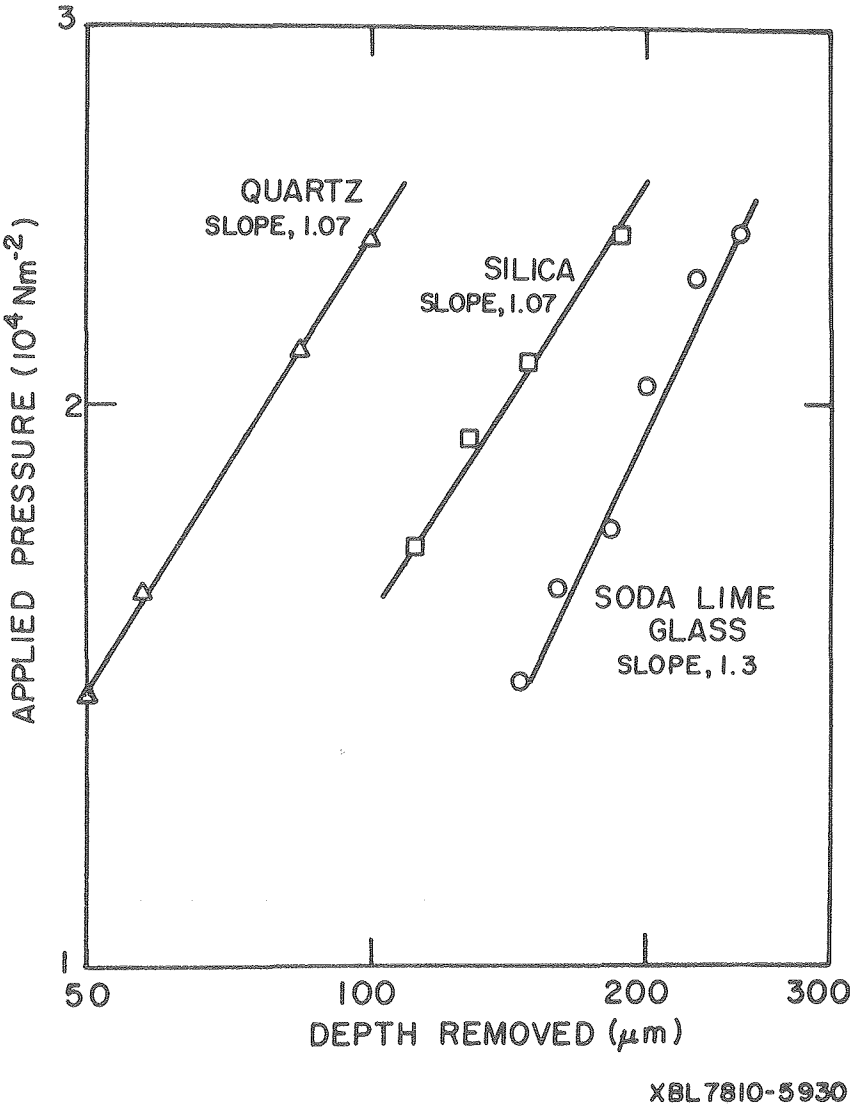


Fig. 4 A plot of the material removed as a function of the applied force[15].

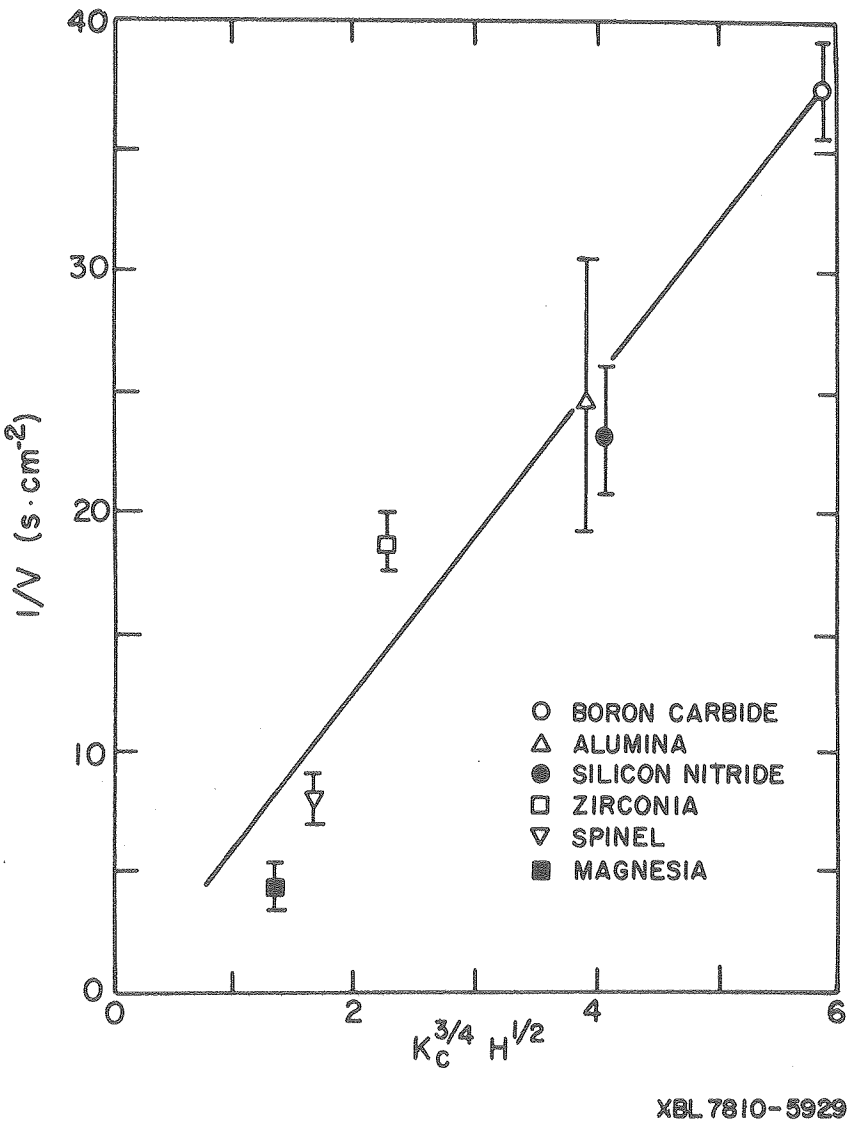


Fig. 5 A plot of the inverse of the material removal against the material dependent parameter $K_c^{2/3}$ $H^{1/2}$ predicted by the lateral fracture analysis.

on the normal force has been explored by Hartley and Wilshaw [15] (Fig. 4). A non-linear force dependence with an exponent ranging between 1.07 and 1.3 was found, similar to the predicted dependence of $P^{7/6}$. The important dependence on the material properties $K_c$ and H can be ascertained from the study of Rice and Speronello [16]. A comparison of their results with the predicted material dependent quantity, $H^{1/2} K_c^{2/3}$, reveals a consistent trend (Fig. 5). However, variations of the instability height with the material type have not been incorporated in the comparison, and these could account for some of the residual trends in the experimental results.

The reasonably good correlation of the available abrasive wear results with the lateral cracking model encourages further study. These studies would include the characterization of lateral cracking under conditions that simulate abrasive wear, and estimations of the zone of material removal vis-a-vis the zone of lateral fracture.

## 3. Other Mechanisms

### 3.1 Thermal stresses

It is widely recognized that heat is generated during a grinding operation. This heat derives primarily from the plastic work expended by the penetration of the abrading particles. An upper bound (adiabatic) estimate of the thermal stresses that develop as a consequence of the heat generation is derived in this section. The potential influence of the thermal stresses upon material removal are then assessed.

The plastic work $W_p$ expended during indentation can be estimated from the macroscopic force-penetration curve, (Fig. 6) as;

$$W_p = \int_0^{\hat{p}} P d\delta_p \tag{16}$$

where $\delta_p$ is the plastic penetration. The plastic penetration is directly related to the contact diameter 2a through the profile of the penetrator. For a penetrator of fixed profile (Fig. 6);

$$\delta_p = a \cot\theta \tag{17}$$

The penetration pressure (i.e. the hardness, H) for a fixed profile indenter is independent of the penetration. Hence, for an axisymmetric penetrator, combining equations (9), (16) and (17) and integrating gives;

$$W_p = \frac{\cot\theta}{3(\beta\pi)^{1/2}} \left[\frac{\hat{P}^{3/2}}{H^{1/2}}\right] \tag{18}$$

It is interesting to note the inverse dependence on the hardness. This arises because the plastic penetration decreases more rapidly with the increase in hardness than the

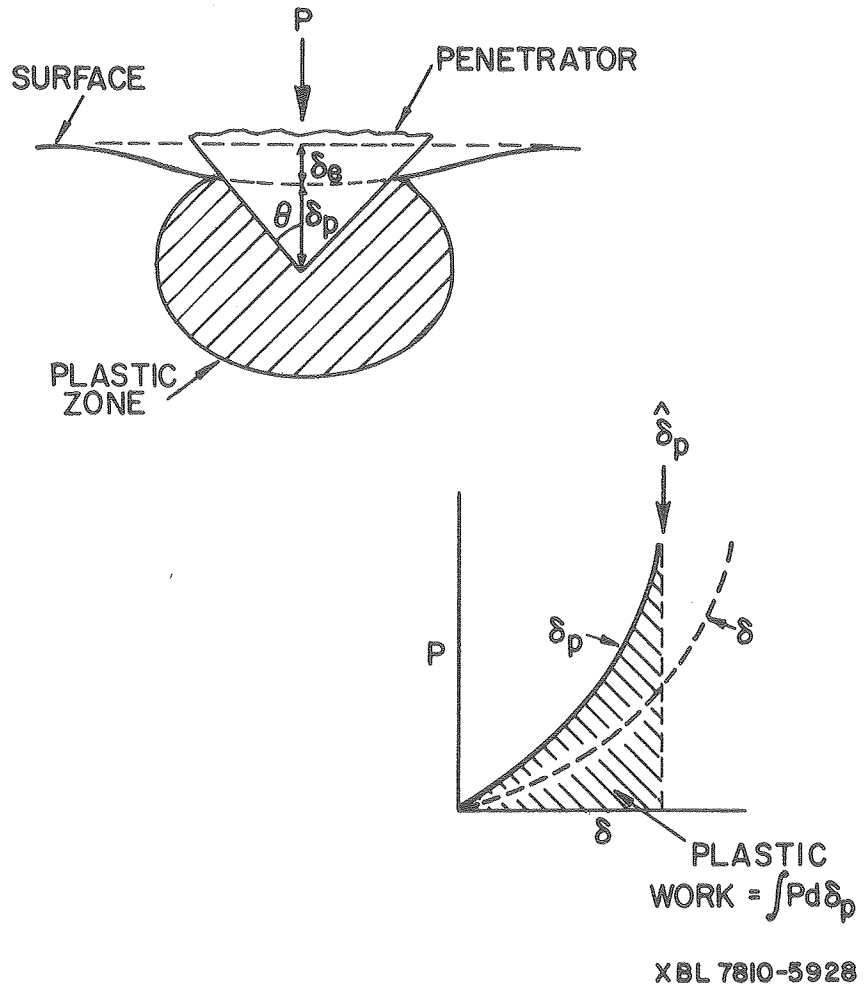


Fig. 6 A schematic indicating the elastic $\delta_1$ and plastic $\delta_p$ penetrations by a fixed profile indenter.

concomitant increase in the penetration force.

The work expended during a lateral traverse of an abrading article depends very sensitively on the details of the traverse. In the presence of instabilities in the lateral motion, individual impacts will occur at various sites along the traverse. The plastic work at each impact site will be given approximately by eq. (18). Under adiabatic conditions, if all of the plastic work is converted into heat, the temperature T generated within the plastic zone at each impact site is;

$$T \approx W_p \left[ (4\pi/3) r_p^3 \rho c_p \right]^{-1} \tag{19}$$

where $c_p$ is the specific heat and $\rho$ is the density. Setting $r_p \approx a$ and combining with eq. (9) then gives;

$$T = \left( \frac{3\ \beta\ \cot\theta}{4} \right) \left( \frac{H}{\rho c_p} \right) \tag{20}$$

Note that the temperature rise is independent of the applied force. Heat flow during penetration will clearly reduce this temperature, as dictated by the differential equation;

$$\frac{d^2T}{dr^2} = \rho \frac{c_p}{k} \left( \frac{dT}{dt} \right) \tag{21}$$

where k is the thermal conductivity.

The local increase in temperature will generate thermal stresses.[†] By assuming the plastic zone to be a spherical enclave in an infinite body (Fig. 7), the thermal stresses are analogous to the stresses that develop due to thermal expansion mismatch [17], viz,

$$\left.\begin{aligned} \sigma_{rr} &= -\frac{2E\alpha T}{3(1-\nu)} \left( \frac{r_p}{r} \right)^3 \\ \sigma_{\theta\theta} &= \frac{E\alpha T}{3(1-\nu)} \left( \frac{r_p}{r} \right)^3 \end{aligned}\right\} \qquad (r > r_p)$$

$$\sigma_{rr} = \sigma_{\theta\theta} = -\ 2E\alpha T/3(1-\nu) \qquad (r < r_p) \tag{22}$$

where r is the distance from the center of the plastic zone. An upper bound value for the tensile stress generated by the local plasticity, obtained from eqs. (20) and (22) is thus;

---

[†]An elastic solution is not strictly valid, because the thermal shear stresses, which are a maximum at $r_p$, superimpose on the penetration stresses and extend the plastic zone.

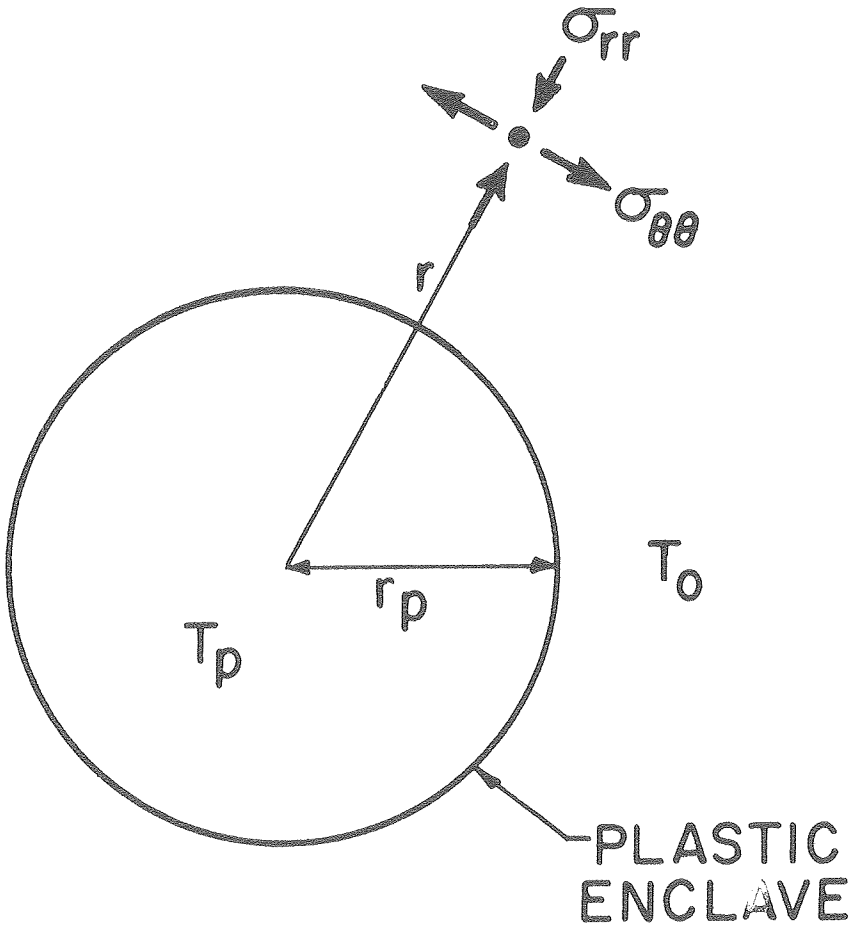


Fig. 7 A plastic enclave in an elastic matrix indicating the stresses developed by heat genration in the plastic zone.

$$\hat{\sigma}_{\theta\theta} = \frac{\beta \cot\theta}{4(1-\nu)} \left(\frac{\alpha H E}{\rho c_p}\right) \tag{23}$$

Inserting some typical values for E, $\rho$, $c_p$ and $\alpha$ into eq. (23) yields values of $\hat{\sigma}_{\theta\theta}$ in the range $\sim 10^{-2}$ to $10^{-1}$H. These stresses approach the stresses that result from plastic penetration (eq. 4). Thermal stresses should thus be regarded as a possible source of material removal, particularly in materials with large values of thermal expansion coefficients, elastic modulus and hardness, and low values of specific heat. Since the thermal stresses are independent of the normal force, the thermal influences should be particularly effective at low force levels. The thermal stresses could either enhance the lateral fracture just above the threshold force P*, or perhaps, provide an independent mechanism of material removal below P*.

### 3.2 Elastic stress pulses

Impact events can, in certain situations, lead to the generation of Rayleigh waves [18]. The Rayleigh wave can produce large amplitude, short duration tensile pulses, which introduce circumferential cracks that link together to cause material removal [19]. A similar mechanism could apply in abrasive wear, under analogous circumstances, e.g., the wear of very hard materials at low force levels. An important feature of this mechanism is that crack development is impeded by large values of the elastic wave velocity.

## 4. Summary

Some mechanisms of material removal during abrasive wear have been assessed. A preliminary lateral fracture model has been developed. The model indicates that a minimum force is required to initiate lateral fracture. The threshold force is determined primarily by the fracture toughness and the hardness.

The material removal that occurs by lateral fracture above the threshold has been estimated to depend on the normal force, the hardness and toughness as well as on the the lateral velocity and friction coefficient (through local instabilities caused by the fracture process). A comparison of the predictions that emerge from the preliminary model with available data indicates encouraging correlations. Further development of lateral fracture models thus appear to be a promising course for future studies of abrasive wear.

An upper bound estimate of the thermal stresses that result from plastic grooving indicates that these stresses can be appreciable. The stresses are, to a first approximation, independent of the normal force, suggesting that the thermal stresses are likely to be most important at low force levels, i.e., when the lateral fracture mechanism is least effective. The thermal stresses are enhanced by large values of the thermal expansion coefficient, elastic modulus and hardness and small values of the specific heat. Thermal effects are most likely to emerge in materials with these properties. Thermal stresses can either enhance the extent of lateral fracture just above the threshold, or provide

an alternate material removal mechanism.

Finally, one other mechanism has been suggested, by analogy with impact problems. It entails the growth of cracks by elastic tensile stress pulses generated by deformable particles. However, no specific estimates of the realm of importance of this mechanism have yet been obtained.

## ACKNOWLEDGEMENT

This work was supported in part by the Office of Naval Research and in part by the Division of Materials Sciences, Office of Basic Energy Sciences, U.S. Department of Energy.

## REFERENCES


[1] Gielisse, P. J. and Stanisloa, J., The science of ceramic machining and surface finishing, NBS Special Technical Publication, [348], 5, (1972).

[2] Swain, M. V., Fracture mechanics of ceramics (Ed. Bradt, R. C., Hasselman, D.P.H. and Lange, F. F.), Plenum, NY, 3, 257, (1978).

[3] Veldkamp, J.D.B., Hattu, N. and Snyders, V.A.C., Fracture mechanics of ceramics, 3, 273, (1978).

[4] Evans, A. G. and Wilshaw, T. R., Acta Met., [24], 939, (1976).

[5] Evans, A. G., Gulden, M. E. and Rosenblatt, M., Proc. Royal Soc., [A361], 343, (1978).

[6] Lawn, B. R. and Wilshaw, T. R., Journal of Mater. Sci., [10], 1049, (1975).

[7] Swain, M. V., and Hagan, J. T., Jnl. Phys., [9], D, 2201, (1976).

[8] Evans, A. G., ASTM Special Technical Publication, in press

[9] Perrott, C.M., Wear, [45], 293, (1977).

[10] Tabor, D., Hardness of Metals, Oxford: Clarendon Press, (1951).

[11] Lawn, B. R. and Evans, A. G., Jnl. Mater. Sci. [12], 2195, (1977).

[12] Lankford, J., to be published.

[13] Hamilton, G. M., and Goodman, L. E., Jnl. Appl. Mech., [33], 371, (1966).

[14] Evans, A. G. and Charles, E. A., Jnl. Amer. Ceram. Soc., [59], 371, (1976).

[15] Wilshaw, T. R. and Hartley, N.E.W., (Proc. Third European Symposium on Comminution), Chemia GMBH, Weinheim/Bergestrasse, (1972).

[16] Rice, R. W. and Speronello, B. K., Jnl. Amer. Ceram. Soc., [59], 330, (1976).

[17] Selsing, J., Jnl. Amer. Ceram. Soc., [44], 419, (1961).

[18] Evans, A. G., Treatise on materials science and engineering, (Ed. Preece, C.M.), Academic Press, in press.

[19] Adler, W. F., Jnl. Mater. Sci., [12], 1253, (1977).

This report was done with support from the Department of Energy. Any conclusions or opinions expressed in this report represent solely those of the author(s) and not necessarily those of The Regents of the University of California, the Lawrence Berkeley Laboratory or the Department of Energy.

TECHNICAL INFORMATION DEPARTMENT
LAWRENCE BERKELEY LABORATORY
UNIVERSITY OF CALIFORNIA
BERKELEY, CALIFORNIA 94720